

## Luminescence decay times of KBr:Ga<sup>+</sup>

D. Le Si Dang, R. Romestain, and D. Simkin\*

*Laboratoire de Spectrométrie Physique,<sup>†</sup> Université Scientifique et Médicale de Grenoble, Boîte Postale 53, 38041 Grenoble Cedex, France*

A. Fukuda

*Tokyo Institute of Technology, Department of Textile and Polymeric Materials, Meguro-ku, Tokyo 152, Japan*

(Received 16 July 1976)

The kinetics of the luminescent decay of KBr:Ga<sup>+</sup> have been studied from 1.6 to 300 K. Below 45 K, a complex decay consisting of a slow ( $\tau_s$ ) and fast ( $\tau_f$ ) time constant is observed for both the  $A_T$  and  $A_X$  emissions. The temperature dependence of the  $A_T$  and  $A_X$  decay is explained in terms of the same model: in both  $A_T$  and  $A_X$  the emitting levels are twofold degenerate with a nondegenerate trap below, in agreement with recent calculations of Bacci *et al.* and Fukuda *et al.* From 45 to 55 K, the decay time  $\tau_s$  of  $A_T$  is found to be equal to the rise time of  $A_X$ . Over the same range of temperature, the  $A_X$  emission increases at the expense of the  $A_T$  emission. Analysis of these data shows that  $A_T$  and  $A_X$  relaxed excited states are actually connected by a nonradiative process involving an activation energy  $B$ .

### I. INTRODUCTION

In alkali halides containing heavy-metal ions with outer electronic configuration  $ns^2$  such as Ga<sup>+</sup>, In<sup>+</sup>, Tl<sup>+</sup> one observes typically three absorption bands called  $A, B, C$  in order of increasing energy. An interesting feature observed in most phosphors is that excitation into the  $A$  band ( $^1A_{1g} \rightarrow ^3T_{1u}$ ) yields two emission bands designated as  $A_T$  (high energy) and  $A_X$  (low energy). Fukuda<sup>1</sup> explained the emission spectra by assuming that  $A_T$  and  $A_X$  emissions would occur from two types of minima coexisting on the  $^3T_{1u}$  adiabatic-potential-energy surface (APES). As shown by Ranfagni,<sup>2</sup> Bacci *et al.*,<sup>3</sup> and Fukuda *et al.*,<sup>4</sup> coexistence of two kinds of minima on the  $^3T_{1u}$  APES is allowed when considering (i) mixing effects with the higher  $^1T_{1u}$  excited states due to large spin-orbit interaction<sup>2</sup> or (ii) bilinear terms in the electron-lattice interaction.<sup>3,4</sup> The symmetry and the energy-level structure of the two minima depend on the situation considered (for more details see Ref. 3). For Ga<sup>+</sup> situation (ii) seems to be appropriate since its spin-orbit interaction is small with respect to the exchange energy. In that case, one would expect a level structure for Ga<sup>+</sup> consisting of a doubly degenerate level with a trap below for both  $A_T$  and  $A_X$  minima. We have undertaken the present study of the kinetics of the KBr:Ga<sup>+</sup> fluorescence in the hope of obtaining infor-

mation about the level structure of the  $A_T$  and  $A_X$  emissions.

### II. EXPERIMENTAL

Emission was excited by illuminating into the  $A$  absorption band at 270 nm using a uv filter and either a deuterium flash lamp (TRW Model 88A) or a high-pressure oxygen flash lamp.<sup>5</sup> The deuterium lamp gave pulses of about 5-nsec duration, while those of the oxygen lamp were about 100 nsec. Decay times measured with both lamps were in complete agreement, but much higher intensities were possible with the oxygen lamp. The  $A_T$  or  $A_X$  emission was then selected by a broadband filter (centered at 450 nm for  $A_T$  and 550 nm for  $A_X$ ) and measured with an EMI 9558 QB photomultiplier. The data were stored in a multichannel analyzer with a minimum channel width of 200 nsec. Regulated temperatures from 1.2 to 300 K were obtained with a gas flow cryostat. Temperatures were measured with a calibrated germanium resistance.

The results of the lifetime measurements of the  $A_X$  and  $A_T$  emissions after  $A$  excitation are shown in Figs. 1 and 2. As seen in Fig. 1, one observes a drastic change in the decay of  $A_T$  at 45 K. Thus, one can distinguish in the kinetics of the  $A_T$  and  $A_X$  decays a low-temperature part (for temperatures below 45 K)

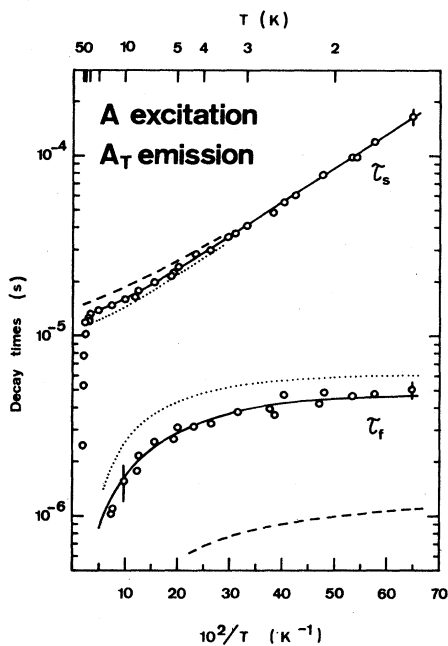


FIG. 1. Temperature dependence of the slow ( $\tau_s$ ) and fast ( $\tau_f$ ) time constants of the  $A_T$  decay. Best fits to the experimental data obtained with Eq. (5) and under the assumption of a one-phonon relaxation process between levels 1 and 2 are shown for different ratios of the degeneracies  $g_2$  to  $g_1$ :  $g = g_2/g_1 = 1$  (curve, broken line), 2 (curve, solid line), 3 (curve, dotted line).

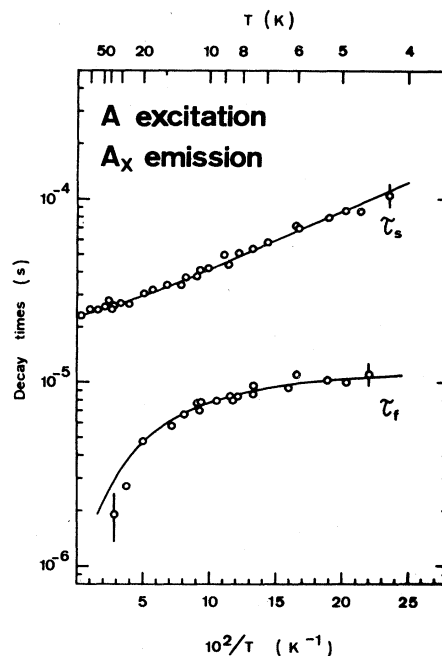


FIG. 2. Temperature dependence of the slow ( $\tau_s$ ) and fast ( $\tau_f$ ) time constants of the  $A_X$  decay. Best fit to the experimental data obtained with Eq. (5), under the assumption of a one-phonon relaxation process and for  $g = g_2/g_1 = 2$ , is given by the solid line.

and a high-temperature part (for temperatures above 45 K).

### III. KINETICS OF THE FLUORESCENCE BELOW 45 K

#### A. Energy-level structure

Below 40 K the intensities of  $A_T$  and  $A_X$  emissions are temperature independent (see inset in Fig. 3). Thus, one can reasonably assume that the relaxed excited states of  $A_T$  are disconnected from those of  $A_X$  over the low-temperature range. On the other hand, the fluorescence kinetics of  $A_T$  and  $A_X$  behave in qualitatively the same fashion: both decays are characterized by two time constants  $\tau_s$  and  $\tau_f$  (see Figs. 1 and 2). This suggests that, as expected theoretically,<sup>3,4</sup> the same kinetic model involving only two sets of levels should apply for both fluorescence decays of  $A_T$  and  $A_X$ .

Our kinetic model is shown in Fig. 4. In the figure there is a group of levels, labeled 1, with a probability for radiative transition to the ground state  $k_1$ . A second group of levels, 2, is located at energy  $D$  above 1, and has a radiative transition probability for decay

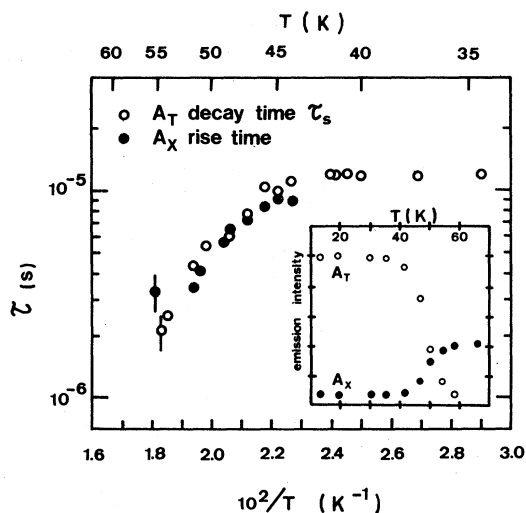


FIG. 3. Temperature dependence of the decay time  $\tau_s$  of the  $A_T$  emission and the rise time  $\tau$  of the  $A_X$  emission. The inset shows the temperature dependence of the  $A_T$  and  $A_X$  emissions.

to the ground state of  $k_2$ . The ratio of the degeneracies  $g_2/g_1$  of the two groups of levels is called  $g$ . The nonradiative transition from  $2 \rightarrow 1$  occurs with a probability  $k_{21}$ , while the reverse process has a probability

$$k_{12} = k_{21} \exp(-D/kT) .$$

This model then gives the following rate equations:

$$\frac{dN_2}{dt} = -(k_{21} + k_2)N_2 + gk_{12}N_1 , \quad (1)$$

$$\frac{dN_1}{dt} = k_{21}N_2 - (gk_{12} + k_1)N_1 , \quad (2)$$

where  $N_2$  and  $N_1$  are respectively, the populations of levels 2 and 1 at any time. These equations have the solutions

$$N_2(t) = A_s \exp(-t/\tau_s) + A_f \exp(-t/\tau_f) , \quad (3)$$

$$N_1(t) = B_s \exp(-t/\tau_s) + B_f \exp(-t/\tau_f) . \quad (4)$$

The two roots of the quadratic equation

$$[gk_{12}k_2 + k_1(k_{21} + k_2)]\tau^2 - (k_{21} + gk_{12} + k_1 + k_2)\tau + 1 = 0 , \quad (5)$$

give the two observed time constants  $\tau_s$  and  $\tau_f$ .

We assume for the moment that the relaxation process between levels 1 and 2 is a one-phonon process (or direct process), so that  $k_{12} = Kn$ , where  $n$  is the Bose-Einstein distribution function

$$n = [\exp(D/kT) - 1]^{-1} .$$

A value for  $g$  is chosen ( $g = 1, 2, \text{ or } 3$ ). Then there remain four parameters:  $K, k_1, k_2$ , and  $D$ . These four parameters can then be determined from the best fit

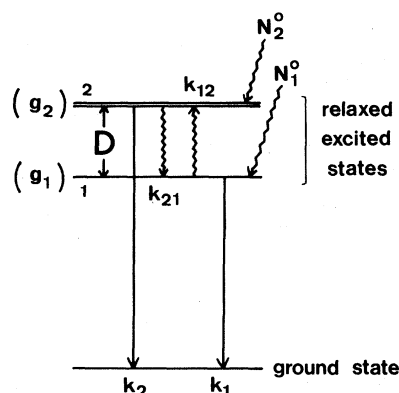


FIG. 4. Energy-level scheme for  $A_T$  and  $A_X$  emissions.  $N_1^0$  and  $N_2^0$  are the initial populations of levels 1 and 2 just after the excitation pulse.  $g_1$  and  $g_2$  are the degeneracies of levels 1 and 2. Wavy arrows and straight arrows indicate, respectively, nonradiative and radiative transitions.

to the experimental data:  $\tau_s(T)$  and  $\tau_f(T)$ . The parameter  $k_1$  could be dismissed at once, since at low temperatures  $\tau_s(T)$  showed no tendency to level off, indicating values of  $k_1^{-1} \gg 200 \mu\text{sec}$  for  $A_T$ , and  $k_1^{-1} \gg 100 \mu\text{sec}$  for  $A_X$ . The calculated  $\tau_s(T)$  and  $\tau_f(T)$  depended strongly on the value chosen for the ratio  $g$  of the degeneracies. Best fit to the data was obtained with  $g = 2$  (solid lines in Figs. 1 and 2). For comparison, tentative fits with  $g = 1$  and 3 are also shown in Fig. 1 (dotted lines and broken lines). While an acceptable fit to  $\tau_s$  could be found with  $g = 1$  and 3, neither of these could simultaneously fit  $\tau_s$  and  $\tau_f$  at any temperature. In cases where only the slow component  $\tau_s$  is observed, it is hard to unambiguously decide the degeneracy.<sup>6</sup> Although only the ratio of the degeneracies is obtained ( $g = 2$ ), both relaxed excited states of  $A_T$  and  $A_X$  of  $\text{Ga}^+$  in  $\text{KBr}$  likely consist of a radiative doublet with a metastable singlet below.<sup>3,4</sup> Table I summarizes the parameters which give the best fit to the data. The calculated values of the relaxation time between levels 1 and 2, i.e.,  $(k_{21} + 2k_{12})^{-1}$ , at  $T = 2$  and 20 K are given also in Table I. They show that at low temperatures, radiative transitions to the ground state occur before thermal equilibrium has been established in both  $A_T$  and  $A_X$  relaxed excited states. In the high-temperature range, when this relaxation time becomes very short with respect to the radiative decay  $k_2^{-1}$ , one measures a purely radiative lifetime

$$\tau_r = [(g + 1)/g]k_2^{-1} = 1.5k_2^{-1} .$$

The possibility of a two-phonon relaxation process has also been considered. However, a Raman process leads to a  $T^7$  temperature law, while a Orbach process gives rise to an even faster temperature dependence, i.e.,  $k_{21} \propto \exp(-\Delta/kT)$ , where  $\Delta$  would be the energy separation to some higher electronic state. Though agreement could be obtained for a given temperature,

TABLE I. Values of the parameters giving the best fit for the data  $\tau_s(T)$  and  $\tau_f(T)$ . Relaxation times between the radiative doublet and the trap below are calculated at  $T = 2$  and 20 K.

	$A_T$	$A_X$
$1/K$ ( $\mu\text{sec}$ )	$12 \pm 2$	$59 \pm 10$
$1/k_1$ ( $\mu\text{sec}$ )	$>200$	$>100$
$1/k_2$ ( $\mu\text{sec}$ )	$8.5 \pm 1$	$15.4 \pm 2$
$D$ ( $\text{cm}^{-1}$ )	$3.0 \pm 0.3$	$3.9 \pm 0.4$
$g = g_2/g_1$	2	2
Calculated relaxation time, i.e., $(k_{21} + 2k_{12})^{-1}$ :		
$T = 2$ K	8.6 $\mu\text{sec}$	48.8 $\mu\text{sec}$
$T = 20$ K	0.89 $\mu\text{sec}$	5.6 $\mu\text{sec}$

neither of these two-phonon relaxation processes gives the rather weak temperature dependence observed.

### B. Relative intensities of fast and slow components—population rates

The intensity ratio of fast component to slow component  $A_f/A_s$ , which can be obtained from the solution (3) of the rate equations, will provide information about the way the levels are populated during the exciting pulse. Since the pulse length is short compared with all the characteristic times involved, the initial populations  $N_1^0$  and  $N_2^0$  of levels 1 and 2 are just proportional to the feeding rates of these levels. Then the ratio  $A_f/A_s$  at time  $t=0$  is given by

$$\frac{A_f}{A_s} = \frac{gk_{12}N_1^0 + (-1/\tau_f + gk_{12} + k_1)N_2^0}{gk_{12}N_1^0 + (-1/\tau_s + gk_{12} + k_1)N_2^0} \quad (6)$$

In Figs. 5 and 6 the solid lines give the calculated temperature dependence of the intensity ratio  $A_f/A_s$  at time  $t=0$ , using the parameters listed in Table I, and assuming different ratios  $N$  of initial populations of levels 2 to 1:  $N = N_2^0/N_1^0$ . Also shown in Figs. 5 and 6 are the measured ratios  $A_f/A_s$  at time  $t=0$ . For the  $A_T$  emission the experimental points follow the calculated curve for  $N=10$  over the temperature range 1.5–20 K (Fig. 5), while for the  $A_X$  emission the data follow the  $N=2$  curve from 4 to 50 K (Fig. 6). This very different behavior of  $A_T$  and  $A_X$  should be em-

phasized. It appears that only the radiative levels of  $A_T$  are effectively populated, while on the other hand the three levels corresponding to the  $A_X$  emission are randomly populated ( $N=g=2$ ), and this is true over a very large range of temperature.

### IV. KINETICS OF THE FLUORESCENCE ABOVE 45 K

At temperatures below 45 K rise times for both  $A_T$  and  $A_X$  emissions are much less than 200 nsec, and thus cannot be measured with our multichannel analyzer. But over a narrow range of temperature (from 45 to 55 K) one can observe a slower rise time in the  $A_X$  emission (the rise time of  $A_X$  emission in KI:Tl<sup>+</sup> has recently been observed by Ishikane.<sup>7</sup> On the other hand, the  $A_T$  decay time  $\tau_s$ , which has reached the steady value  $\tau_r = 1.5k_2^{-1} = 12.8 \mu\text{sec}$ , changes drastically with the temperature for  $T \geq 45$  K. In fact the  $A_X$  rise time and the  $A_T$  decay time  $\tau_s$  are found to be equal as can be seen in Fig. 3. Over the same range of temperature, the intensity of  $A_X$  emission increases while that of  $A_T$  decreases (see inset in Fig. 3). These experimental facts are strong evidence for the occurrence of a nonradiative process connecting  $A_T$  and  $A_X$  at high temperature. Let  $\tau_{nr}$  be the characteristic time of this nonradiative process. Then, for  $T \geq 45$  K, the  $A_T$  decay rate is given by

$$1/\tau_s = 1/\tau_r + 1/\tau_{nr} \quad (7)$$

In the high-temperature range, the intensity of the  $A_T$

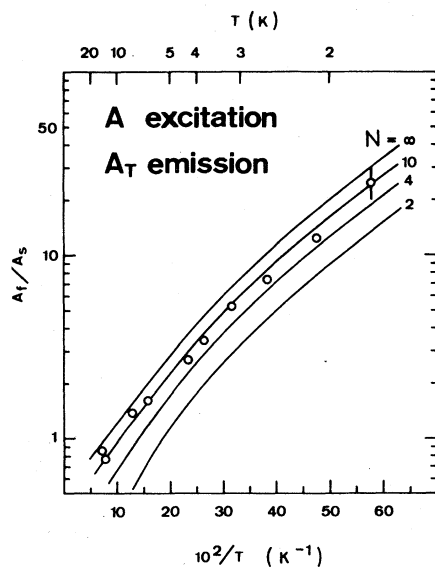


FIG. 5. Ratio of fast component to slow component intensity  $A_f/A_s$  of the  $A_T$  emission. Solid lines are the calculated intensity ratio [Eq. (6)] obtained with the parameters listed in Table I, and for various ratios of initial populations of levels 2 to 1:  $N = N_2^0/N_1^0 = 2, 4, 10, \infty$ .

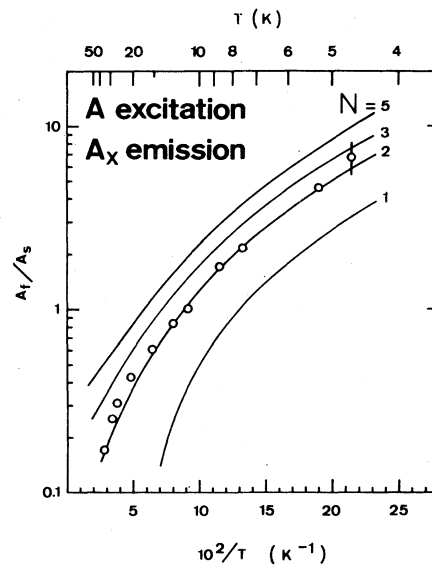


FIG. 6. Ratio of fast component to slow component intensity  $A_f/A_s$  of the  $A_X$  emission. Solid lines are calculated intensity ratio [Eq. (6)] obtained with the parameters listed in Table I, and for various ratios of initial populations of levels 2 to 1:  $N = N_2^0/N_1^0 = 1, 2, 3, 5$ .

emission is related to the radiative decay time by

$$I_0/I = \tau_r/\tau_s \quad (8)$$

where  $I$  and  $I_0$  are, respectively, the  $A_T$  intensity at temperature above and under 45 K. Combining (7) and (8) one gets

$$1/\tau_{nr} = 1/\tau_s - 1/\tau_r = 1/\tau_r(I_0/I - 1) \quad (9)$$

It is found that the  $A_T$  decay time  $\tau_s$  and the  $A_T$  emission intensity  $I$  satisfy relation (8). In fact, the experimental points for both

$$\ln(1/\tau_s - 1/\tau_r), \quad \ln[1/\tau_r(I_0/I - 1)]$$

fall on the same straight line when plotted against  $1/T$  (see Fig. 7), leading to the following expression for the nonradiative process:

$$1/\tau_{nr} = A \exp(-B/kT) \quad (10)$$

where  $A = 8.6 \times 10^{11} \text{ s}^{-1}$ , and  $B = 550 \text{ cm}^{-1}$ .  $B$  is the energy separation between the level  $a$  (see inset in Fig. 7) and the first excited level  $b$  from which a tunneling process towards  $A_X$  potential well becomes effective. This activation energy  $B$  can be either equal to or smaller than the height of the potential barrier between  $A_T$  and  $A_X$  wells on the  ${}^3T_{lu}$  APES. Tunneling from higher levels than level  $b$  in

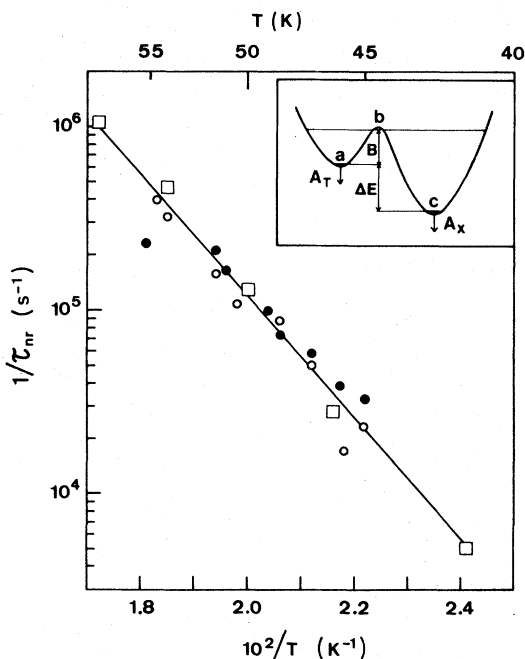


FIG. 7. Temperature dependence of  $1/\tau_{nr}$  [Eq. (9)]: time constants data are shown by open circles (decay time of  $A_T$ ) and full circles (rise time of  $A_X$ ), while open squares represent data on  $A_T$  emission intensity. Inset shows a qualitative cross section of the  ${}^3T_{lu}$  APES.

the temperature range 40 to 60 K seems unlikely, since  $\tau_{nr}^{-1}$  exhibits a single exponential temperature dependence (see Fig. 7). Relaxation between levels  $a$  and  $b$  cannot occur through a one-phonon process, since no phonon of such an energy exists in KBr. Therefore, one has to consider successive absorptions of phonons which allow the system to climb along a "ladder" of vibrational levels defined in the  $A_T$  potential well. Since Raman scattering spectra of  $\text{KBr:Tl}^+$  exhibit strong peaks in the range  $70\text{--}150 \text{ cm}^{-1}$ ,<sup>8</sup> one expects 5–10 intermediate levels between  $a$  and  $b$ . The characteristic rate  $A$  is then a combination of relaxation rates between these levels. The experimental Boltzmann factor takes into account the fact that the whole initial population of the level  $a$  has to go through the level  $b$ , whose population can never be larger than the Boltzmann equilibrium value.<sup>9</sup> As soon as  $\tau_{nr}$  is smaller than the radiative lifetimes  $\tau_r$  of  $A_T$  and  $A_X$ , which are about  $10 \mu\text{sec}$  (see Table I), one obtains a Boltzmann distribution between levels  $a$  and  $c$ . For  $\text{KBr:Ga}^+$ , only  $A_X$  emission is observed at room temperature indicating that  $\Delta E \geq 1000 \text{ cm}^{-1}$ . Finally, it should be noted that there is another mechanism active in populating level  $c$  (from which  $A_X$  emission occurs) other than the one discussed so far, since the  $A_X$  emission intensity is temperature independent in the low-temperature range.

## V. CONCLUSION

The present study of the kinetics of the  $\text{KBr:Ga}^+$  fluorescence is consistent with a model in which: (a) the energy-level structure in both  $A_T$  and  $A_X$  relaxed excited states consists of a radiative doublet with a trap below, (b) after  $A$  excitation, only the radiative doublet is populated in the case of  $A_T$ , while the three levels of  $A_X$  are equally populated, (c) radiative transition to the ground state occurs before thermal equilibrium has been established at  $T \leq 4.2 \text{ K}$  in both  $A_T$  and  $A_X$  relaxed excited states, and (d) for  $T \geq 45 \text{ K}$ ,  $A_X$  minima are mainly populated by a direct transfer from  $A_T$  minima. This transfer actually is due to a nonradiative process involving an activation energy  $B = 550 \text{ cm}^{-1}$ .

As pointed out by Bacci *et al.*<sup>3</sup> and Fukuda *et al.*,<sup>4</sup> coexistence of two types of minima on the  ${}^3T_{lu}$  APES is allowed when including bilinear terms in the electron-lattice interaction. In that case, one would obtain a level structure for both  $A_T$  and  $A_X$  as in (a). However, there remains the problem of the  $A_T$  and  $A_X$  symmetry. The tetragonal symmetry of  $A_T$  has been well established,<sup>10</sup> while that of  $A_X$  is not so certain.<sup>11</sup> Point (b) is consistent with the correlation of linear polarization observed between the  $A$  absorption and the  $A_T$  emission of  $\text{KBr:Ga}^+$ ,<sup>10</sup> which indicates more precisely that one can feed selectively one component of the radiative doublet.

Magnetic circular polarization of emission in various

phosphors has been studied by Fukuda<sup>11</sup>. In particular for KBr:Ga<sup>+</sup> at  $T=4.2$  K, a bump on the circular polarization curve of  $A_T$  is observed at a magnetic field  $H$  of 32 kG when  $H$  is parallel to a [100] axis. Such a bump on the circular polarization curve can be interpreted as due to a level crossing, but only under the condition that thermal equilibrium has not been established in the spin triplet.<sup>12,13</sup> This is exactly the situation of KBr:Ga<sup>+</sup>. Furthermore from our results of a zero-field splitting  $D=3.0 \pm 0.3$  cm<sup>-1</sup>, a level crossing at 32 kG leads to an effective value of  $g \approx 2$ , which is very close to the free spin spectroscopic splitting value. Thus, it can be concluded that the orbital angular momentum is severely quenched as would be the case for a strong Jahn-Teller coupling to  $E_g$  tetragonal modes of vibration in an orbital state  $T_{1u}$ .<sup>14</sup> Such

a situation has been observed with the triplet excited states of  $F$  centers in CaO.<sup>15</sup>

*Note added in proof.* After completion of this work, the optical detection of magnetic resonance in the relaxed excited states  $A_T$  and  $A_X$  has been undertaken in this laboratory.<sup>16</sup> The proposed level structure of  $A_T$  and  $A_X$  has been verified precisely, and their symmetry determined.

#### ACKNOWLEDGMENTS

We would like to thank Dr. Y Merle d'Aubigné for many stimulating discussions. We also thank R. Legras for valuable technical assistance. One of us (D.S.) would like to thank the Direction Générale de la Recherche Scientifique et Technique for support.

\*On leave from McGill University, Dept. of Chemistry, Montreal, Québec, Canada.

†Laboratory associated with the CNRS.

<sup>1</sup>A. Fukuda, Phys. Rev. B **1**, 4161 (1970).

<sup>2</sup>A. Ranfagni, Phys. Rev. Lett. **28**, 743 (1972).

<sup>3</sup>M. Bacci, A. Ranfagni, M. P. Fontana, and G. Viliani, Phys. Rev. B **11**, 3052 (1975).

<sup>4</sup>A. Fukuda, A. Matsushima, and S. Masunaga, J. Lumin. **12**, 139 (1976).

<sup>5</sup>L. Hundley, T. Coburn, E. Garwin, and L. Stryer, Rev. Sci. Instrum. **38**, 488 (1967). This design was modified to permit the use of an external capacitor and thus allow pulses of longer duration and greater power.

<sup>6</sup>K. Kojima, S. Shimanuki, and T. Kojima, J. Phys. Soc. Jpn. **33**, 1076 (1972).

<sup>7</sup>M. Ishikane, Report at the Annual Meeting of the Physical Society of Japan, Kyoto, 1975 (unpublished).

<sup>8</sup>R. T. Harley, J. B. Page, Jr., and C. T. Walker, Phys. Rev. B **3**, 1365 (1971).

<sup>9</sup>J. Cibert and R. Romestain (unpublished).

<sup>10</sup>A. Fukuda, S. Makishima, T. Mabuchi, and R. Onaka, J. Phys. Chem. Solids **28**, 1763 (1967).

<sup>11</sup>A. Fukuda, J. Phys. Soc. Jpn. **40**, 776 (1976).

<sup>12</sup>W. B. Fowler, M. J. Marrone, and M. N. Kabler, Phys. Rev. B **8**, 5909 (1973).

<sup>13</sup>A. Wasiela, G. Ascarelli, and Y. Merle d'Aubigné, J. Phys. Colloq. **34**, C9-123 (1973).

<sup>14</sup>F. S. Ham, Phys. Rev. **138**, A1727 (1965).

<sup>15</sup>P. Edel, C. Hennies, Y. Merle d'Aubigné, R. Romestain, and Y. Twarowski, Phys. Rev. Lett. **28**, 1268 (1972).

<sup>16</sup>Le Si Dang, R. Romestain, Y. Merle d'Aubigné, and A. Fukuda, Phys. Rev. Lett. **38**, 1539 (1977); **39**, 675 (E) (1977).